

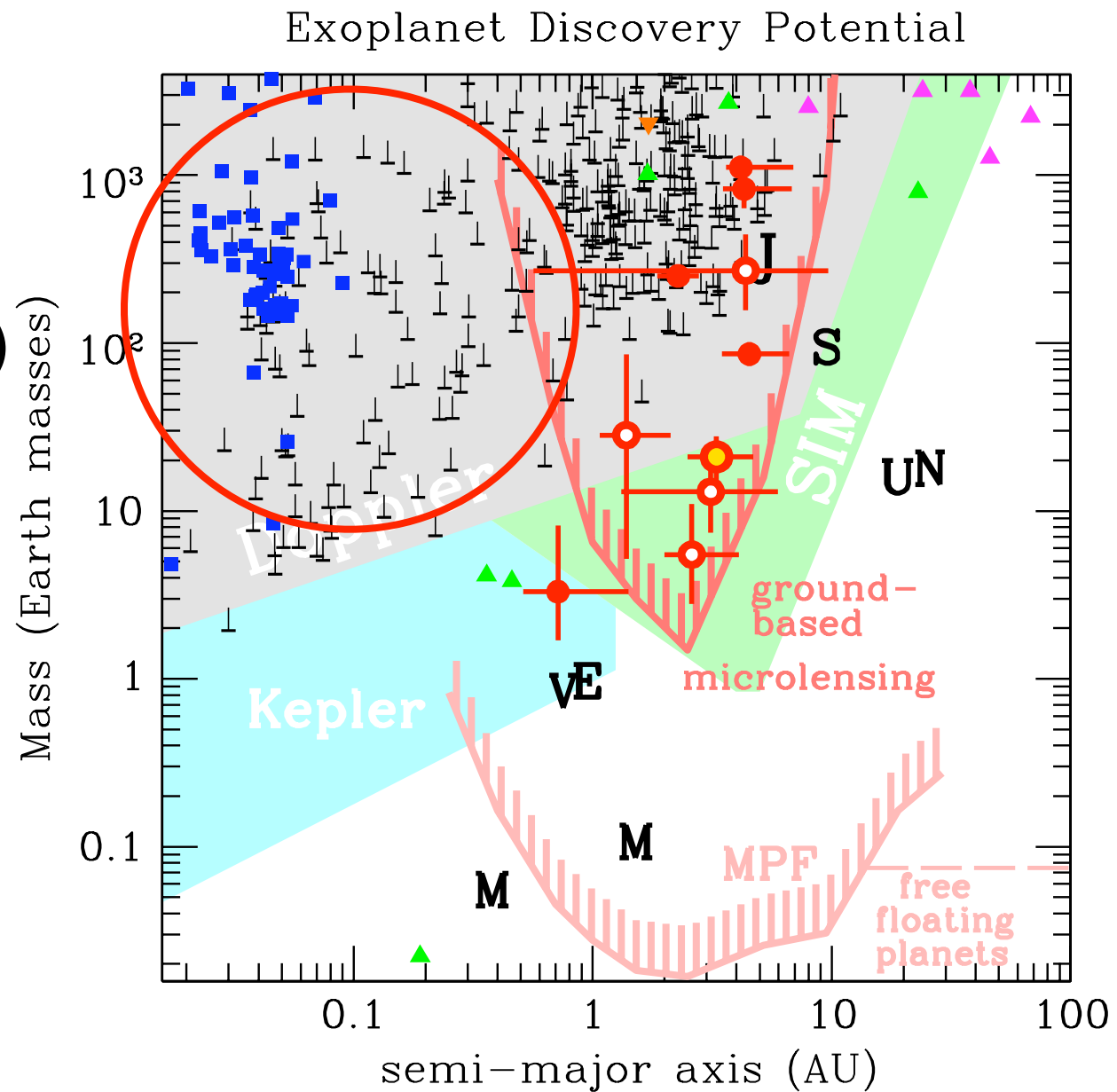
# Unbound or distant planetary mass population detected by gravitational microlensing

# 系外惑星

大部分が

- 小軌道半径
- 木星程度の質量( $M_j$ )

木星質量は地球質量の  
300倍、太陽の $1/1000$



# 系外惑星

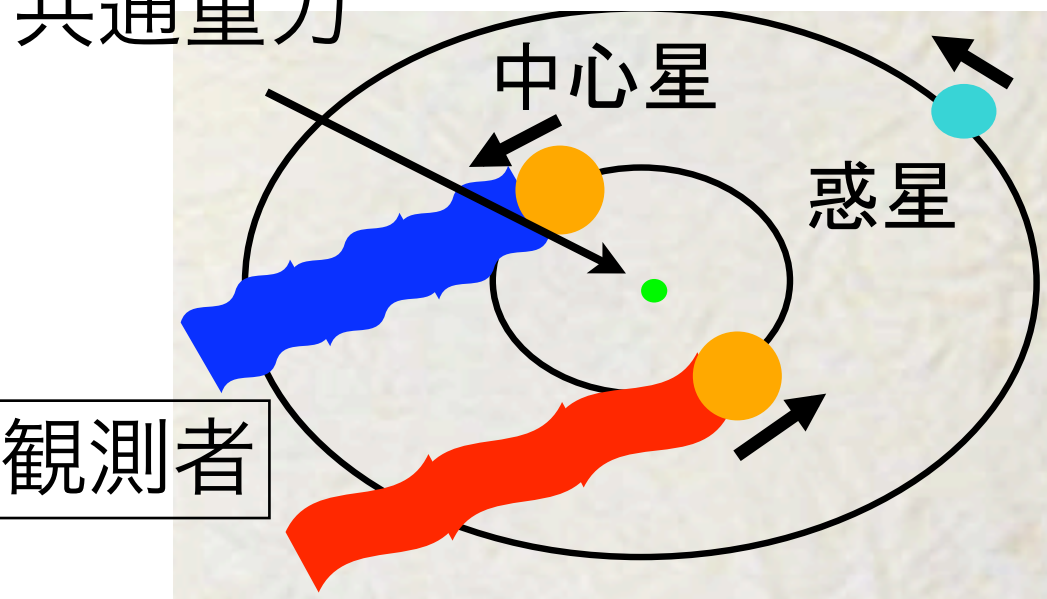
- 現在は500個以上の太陽系以外の惑星(系外惑星)が発見
  - ほとんどが恒星(主星)の周りを回る
- 特定の恒星の周りを回らず宇宙空間を浮遊する「浮遊惑星」は理論的には予想されていたが、観測は困難。
- 日本とニュージーランドの共同研究グループMOAが「重力マイクロレンズ」現象による観測を実現。

**増光期間が1~2日の短い現象を確認→木星質量程度の浮遊惑星を多数発見**

# 系外惑星の検出：ドップラーシフト法

- 共通重力を中心に、惑星だけでなく中心星も公転している。
- 観測者は公転運動を視線(奥行き)速度の変化として捕らえる。
- 視線速度に応じて中心星からの光がドップラー偏移を起こす。その際の波長の変化を捕らえる。

共通重力

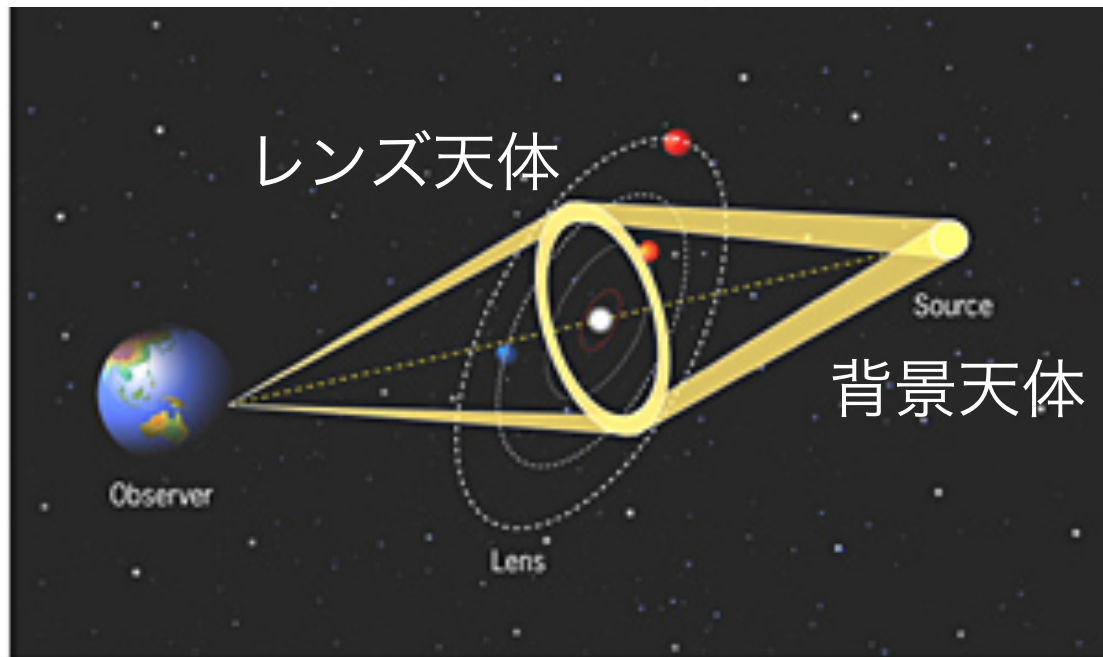


1995年、マイヨールらはこの手法を用いてペガス座51番星に初めて系外惑星を発見した。

中心星に近い重い惑星の探索に向いている。

# 重力マイクロレンズ効果

- 「光が重力によって曲がる」～アインシュタイン一般相対性理論～
- レンズとなる惑星の重力によって背景の星の光が収束・増光
  - 天体が多重像を作ったり(強い重力レンズ)、見かけの形状が変形したり(弱い重力レンズ)はしない。
  - 暗くて見えない遠方の天体に対して有効



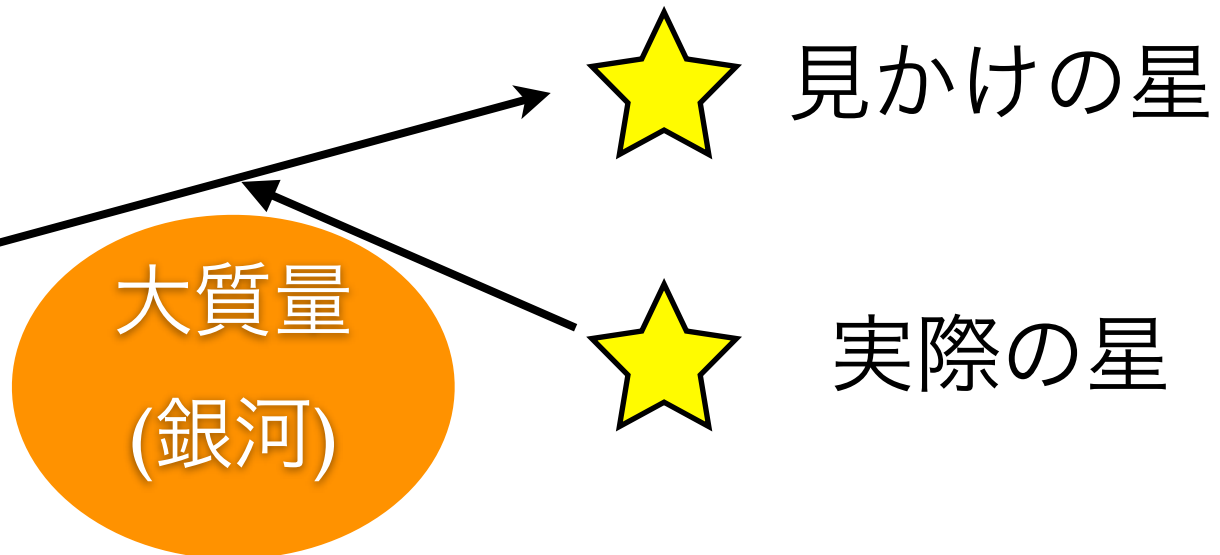
- ダークマター探索(MACHO)
- 太陽系外惑星探索

小口径望遠鏡や普通の観測環境でも十分研究できる

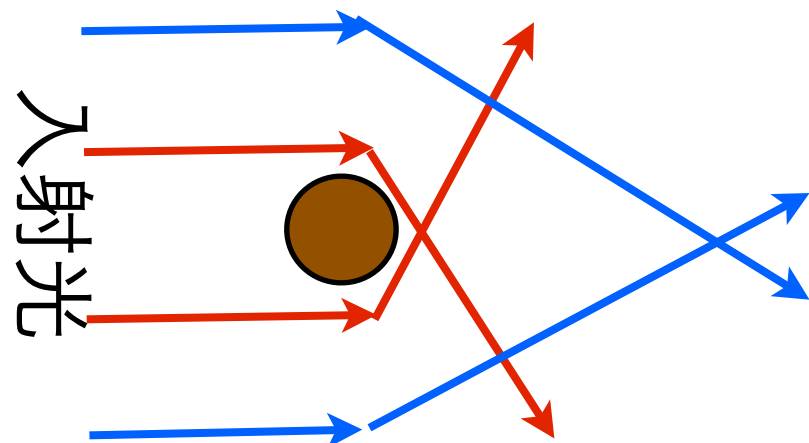
# 重力マイクロレンズ

重力レンズ

観測者



重力レンズは物体(質量)に近いところほど大きく光を曲げる。



質量が小さい場合、上のような屈折(見かけの像の変形)はないが、届かなかつた経路の光が観測者に届くことで増光する → 重力マイクロレンズ

# 発見された木星質量の浮遊惑星イメージ

惑星自体は恒星からの光がないため非常に暗い

<http://www.gcoe.phys.nagoya-u.ac.jp/content0911.html>



Credit: NASA/JPL-Caltech/R. Hurt

# 重力マイクロレンズ効果

$$t_E = \frac{1}{V_t} \sqrt{\frac{4GM}{c^2} \frac{D_L}{D_S - D_L}}$$

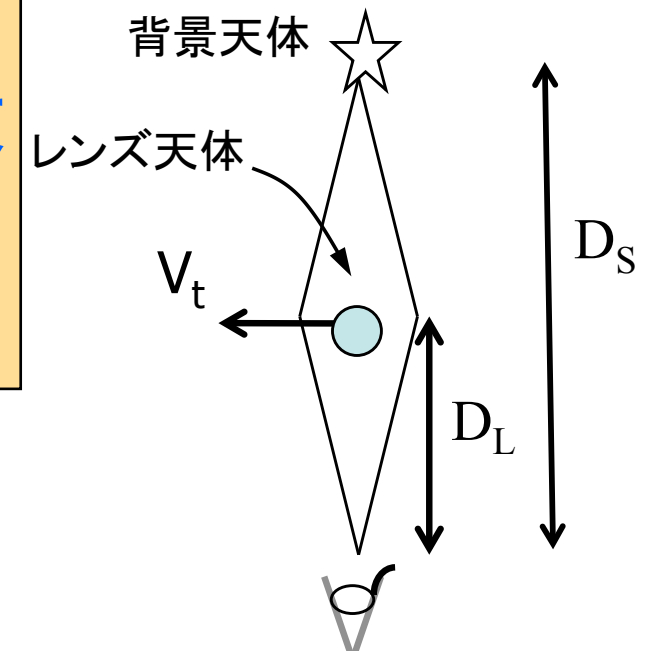
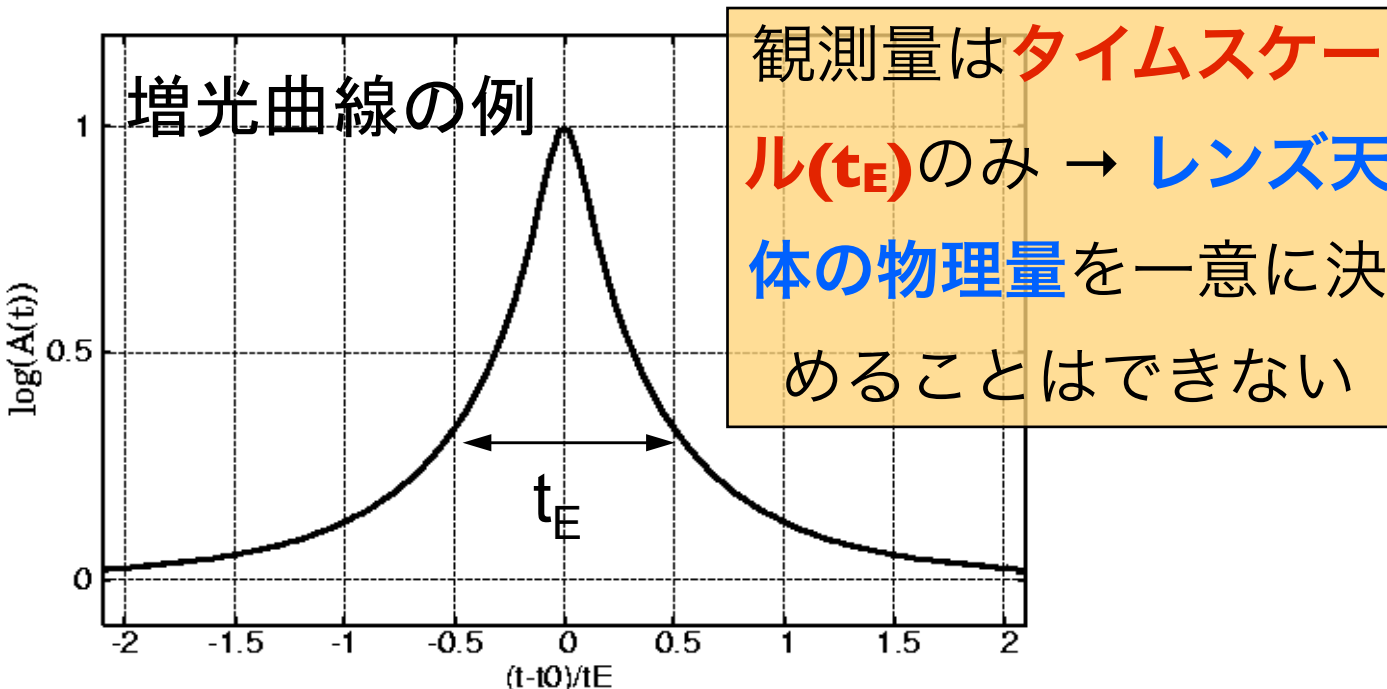
=  $R_E$  (インシュタイン半径)  
 $10\text{AU} \times \left(\frac{M}{M_\odot}\right)^{1/2} \left(\frac{D_S}{50\text{kpc}}\right)^{1/2} \left(\frac{a(1-a)}{1/4}\right)^{1/2}$   
 $a = D_S/D_L$

$$A[x(t)] = \frac{x^2 + 2}{x(x^2 + 4)^{1/2}}$$

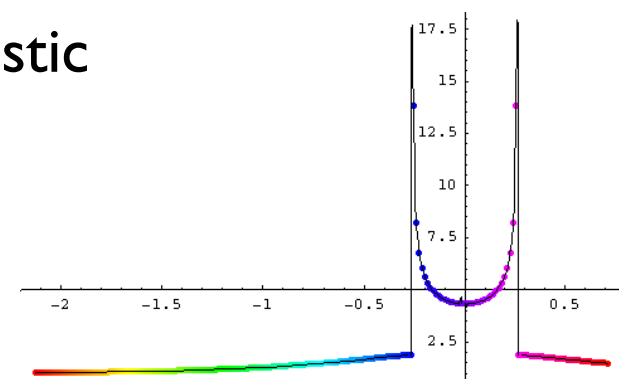
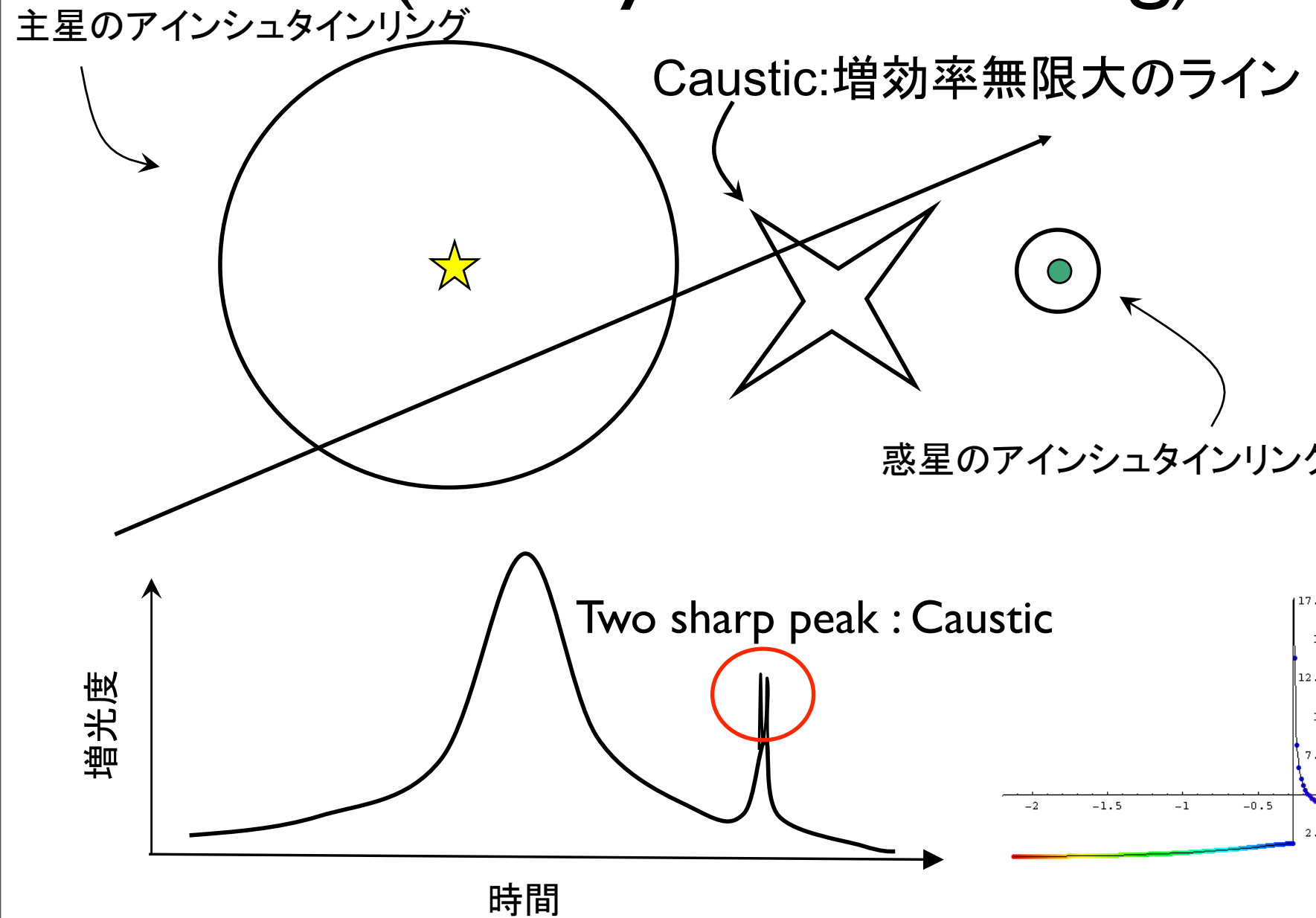
A:増光率  
 b:impact parameter  
 $t_0$ :極大のt

$$x = (b^2 + ((t - t_0) / t_E)^2)^{1/2}$$

- $V_t$  : 速度
- $D_L$  : 距離
- $M$  : 質量

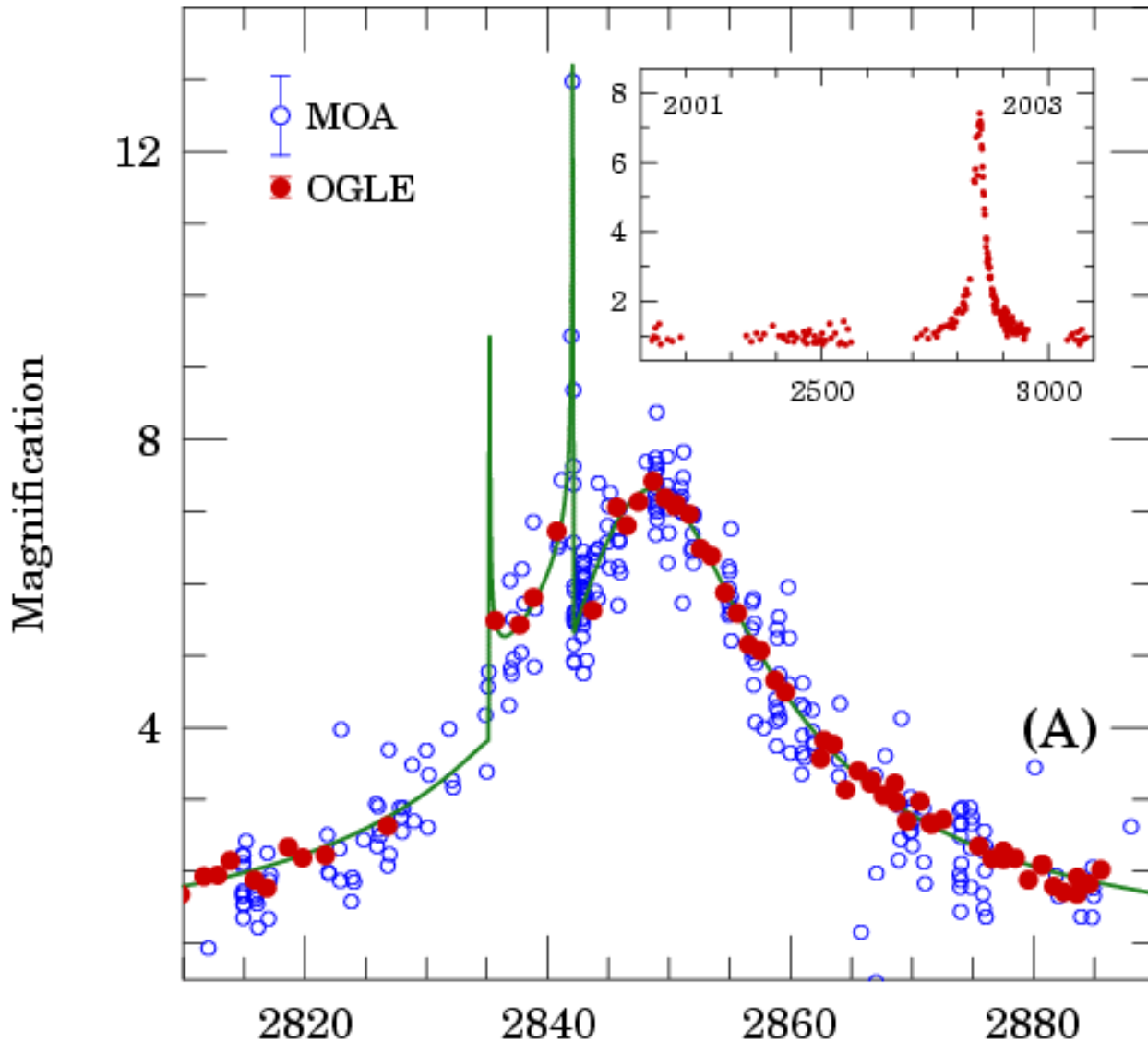


# 連星重力レンズ効果 (Binary microlensing)



# 重力マイクロレンズ(連星)による世界

## 初の系外惑星の検出



OGLE-2003-BLG-235/  
MOA-2003-BLG-53

(A)

伊藤好孝 「重力マイクロレンズ効果による暗天体」

# 重力マイクロレンズによる 増光の特徴

- 波長によらない
- 増光曲線は時間に対して対称
- 同じ天体に対して一度しか増光しない → 追測定が困難。
  - 他地点からのリアルタイムの追測定が必要

## 主なバックグラウンドイベント

- 激変星(CV:Cataclysmic Variable)
  - 短期間(長くて数日)で急激に明るくなり次第に暗くなる星。不規則にこれを繰り返したり、1回だけの場合もある
  - 例：超新星(Supernova)

# MOA Project

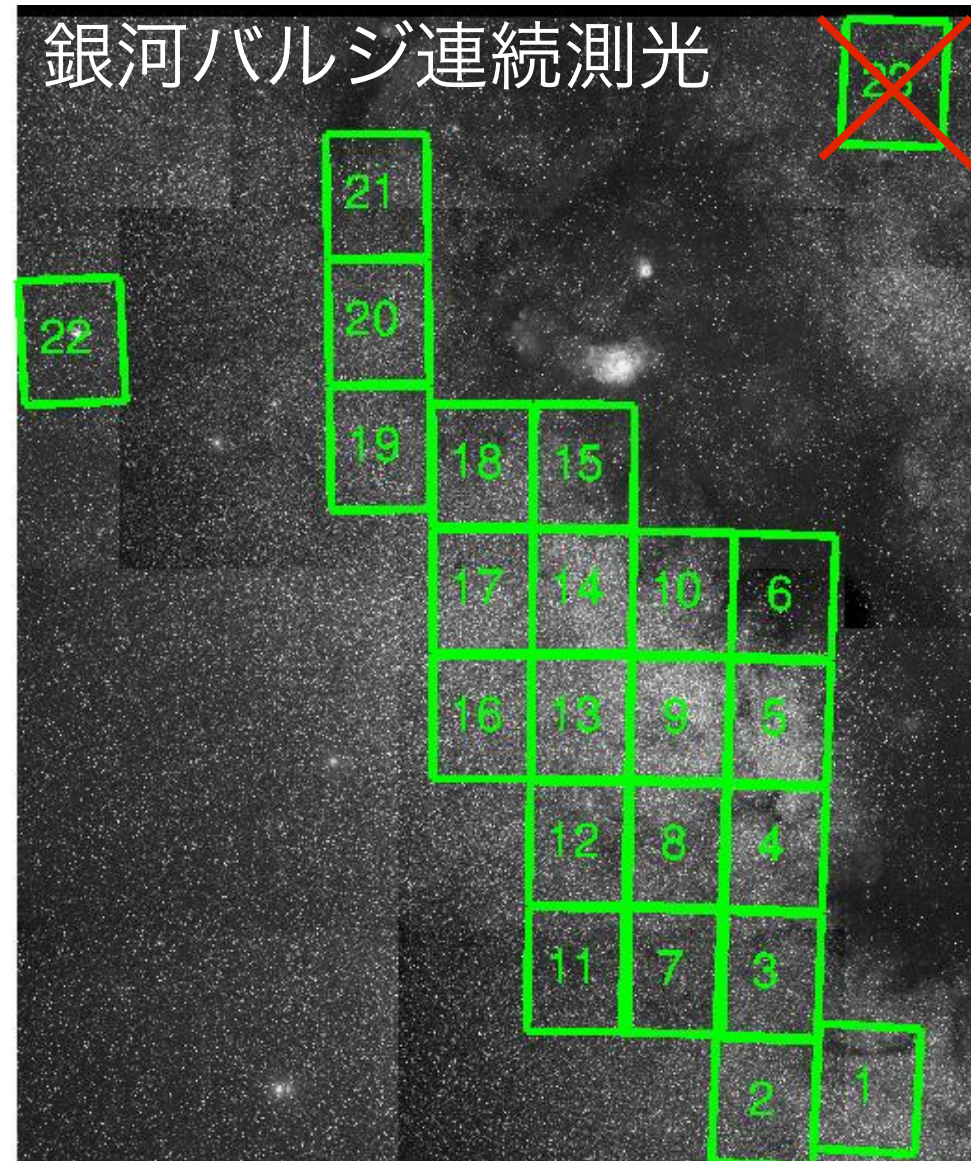


- 重力マイクロレンズ効果により暗い星を観測
- 暗い星：褐色矮星などのダークマター候補天体、太陽系外惑星、ブラックホールなど
- ニュージーランド南島のマウントジョン天文台
- 2004年から1.8m新望遠鏡(MOA-II)による観測を開始。



# Survey toward Galactic Bulge

- 60sec exposure GB5,9 every 10min  
(50 exposures/night)
- Other region every 50min
  - Detect short timescale events  
( $t_E < 2$  days)
- 2006-2007 MOA-II data set
- Clear red clamps for determine the distance to the target object
- Custom filter (sum of Kron/Cousin R and I-band = 600~900nm)
  - Magnitude of reference images were calibrated to I-band with OGLE-II photometry map.



伊藤好孝 「重力マイクロレンズ効果による暗天体」

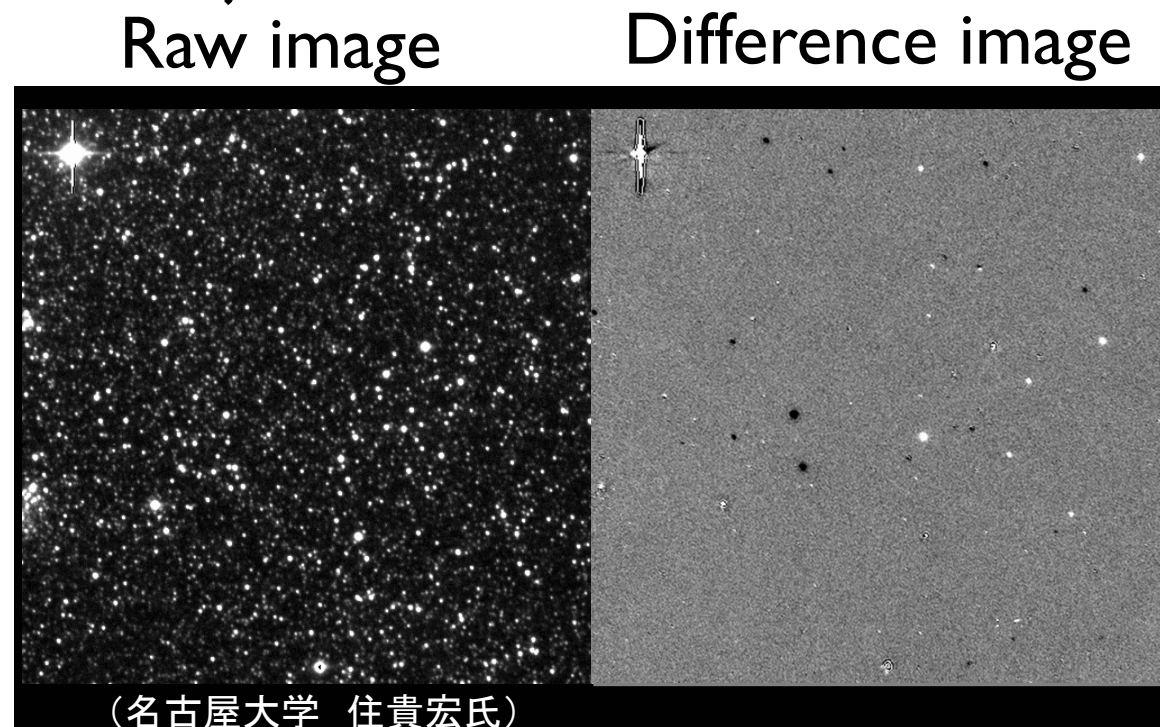
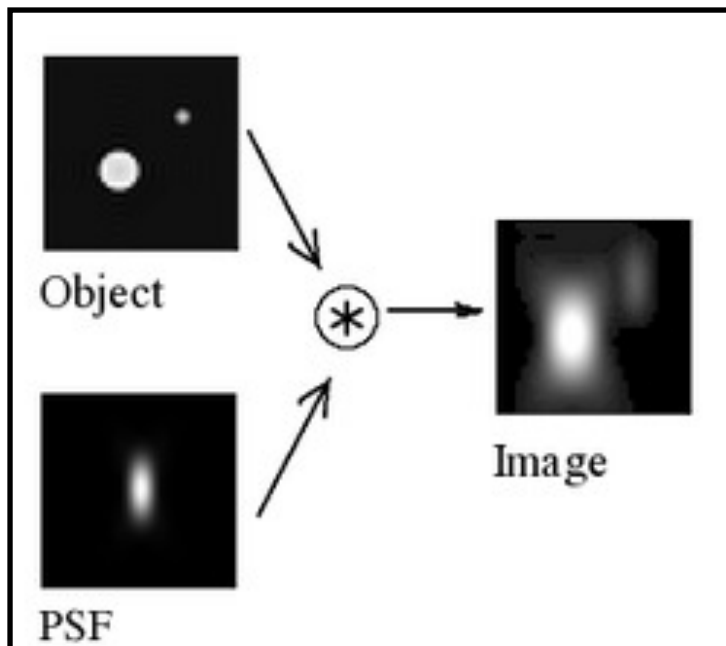
# Event selection

---

level	criteria	comments
cut0	$N_{\text{detect}} \geq 3$	Number of frames in which the object is detected.
cut1	$N_{\text{data}} \geq 500$ $N_{\text{out}} \geq 10$ $\chi^2_{\text{out}}/\text{dof} \leq 3$ $N_{\text{bump}} \geq 1$ $\chi_{3+} = \sum_i (F_i - F_{\text{base}}) / \sigma'_i \geq 80$	Number of data points Number of data points outside of the 120-day window $\chi^2$ outside of the 120-day window Number of bumps in the window, where a bump has $> 3$ consecutive points $> 3\sigma'$ above baseline Total significance of consecutive points with $> 3\sigma'$
cut2	fitting converged $\chi^2/\text{dof} \leq 2$ $\chi_1^2/\text{dof} \leq 2$ $\chi_2^2/\text{dof} \leq 2$ $0.3 \leq t_E \leq 200$ days $\sigma_{t_E}/t_E \leq 0.5$ $\sigma_{t_E} \leq 12$ days $3824 \leq t_0 \leq 4420$ JD' $u_0 \leq 1$ $\sigma_{u_0} \leq 0.3$ $I_s \leq 20.0$ $(F_s - F_{\text{cat}})/F_{\text{cat}} \leq 3$ $\chi_{3+} \geq 70N_{2\sigma} - 500$ $\chi_{3+} \geq 45N_{3\sigma}$ OR $N_{3\sigma} \leq 2$	Fits never converge if parameters are degenerate $\chi^2$ for all data $\chi^2$ for $ t  \leq t_E$ $\chi^2$ for $ t  \leq 2t_E$ Einstein radius crossing timescale Error in $t_E$ Error in $t_E$ Peak should be within observational period The minimum impact parameter Error in $u_0$ Apparent $I$ -band source magnitude Source flux should not greatly exceed catalog flux Exclude systematic residuals (depending on total significance) same as above

# Cut 0

- Subtract background image, Reconstruct variable object as positive or negative PSF (= Point Spread Function, the response of an imaging system to a point source or point object).
- Find difference images from background w/  $S/N > 5$ 
  - Additional criteria to avoid cosmic ray, satellite tracks, electrons leaked from the saturated images of bright stars
- Classify all objects as new one or previously detected.
- Count # of frames of same object  $\rightarrow N_{\text{detect}}$



# Cut I

- Create light curves by PSF fitting photometry on difference images
  - Enough number of signal data in 120-day window.
  - Enough number of pedestal data outside 120-day window. → Define the baseline flux.
- Error bars from calibration with constant stats
- Search for positive light curve “bumps” in 120-day window.

$$Bump = F - F_{base} > 3\sigma'$$

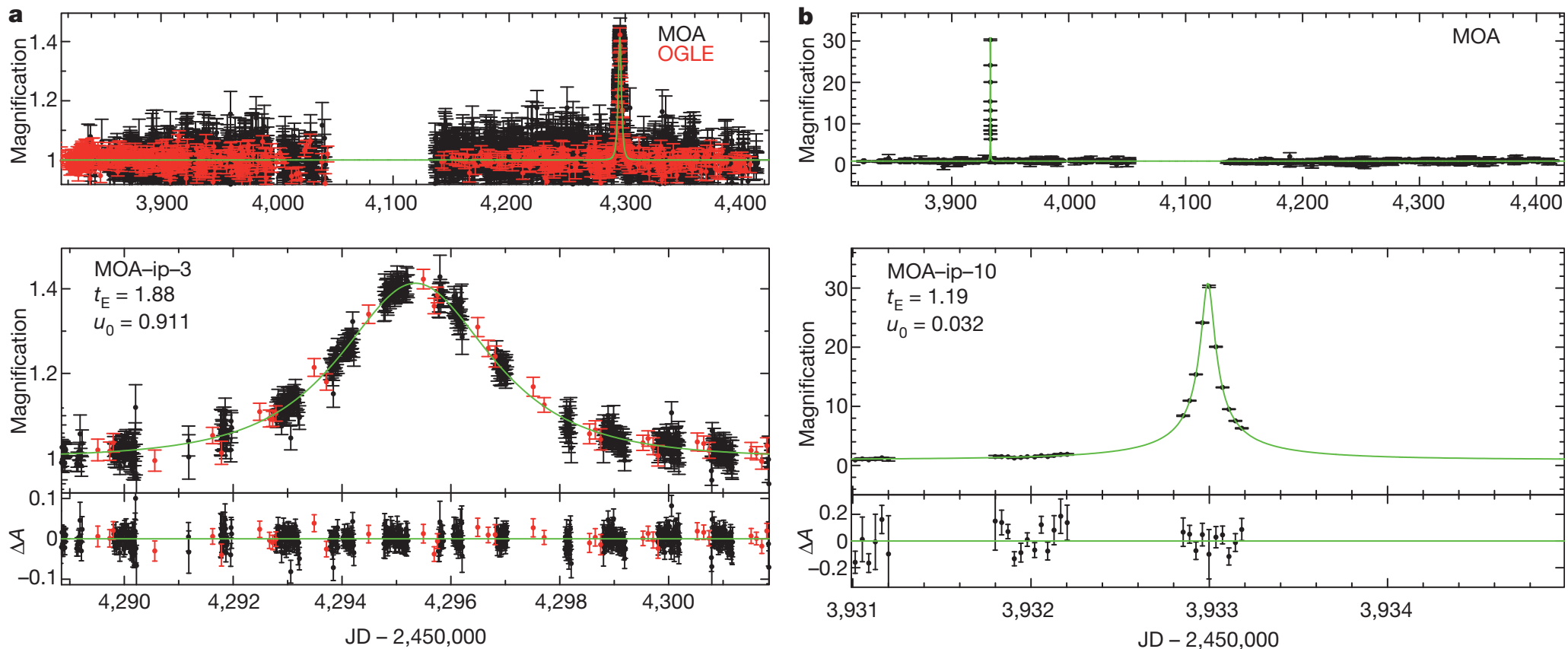
$$\chi_{3+} = \sum_i (F_i - F_{base})/\sigma'_i \text{ with } F_i - F_{base} > 3\sigma'_i$$

# Cut 2

- Fit light curve of “bumps” events with 5-parameter microlensing model assuming a point source and **single lens object**.
  - 5-parameter :
    - $t_E$  : Einstein radius crossing time
    - $t_0$  : time peak magnification
    - $u_0$  : source-lens impact parameter
    - $F_s, F_b$  : source and baseline fluxes
  - More than a thousand microlensing candidates in this data set, only 474 high quality microlensing events have passed our relatively strict criteria

# Light curve of short microlensing events

10 candidates of short timescale ( $t_E < 2$  days) single microlensing events



Green line : best-fit microlensing model

# Back ground

- **Cosmic ray hit**
- Fast Moving object
- **Cataclysmic variables (CVs)**
  - **Supernovae**
- **Binary microlensing events**
- Microlensing by high velocity stars and Galactic halo stellar remnants

# Cosmic-ray hits

- Rare for cosmic ray hits to give a signal with the same profile as the observed PSF
  - Reject cosmic-ray hits by lack of a PSF-like shape.
- Require hit the same place in four consecutive images → Reject
- Each of our 10  $t_E < 2$  day events have at least 10 observations at significant magnification, so there is no chance of contamination by cosmic ray hits.

# Cataclysmic variables (CVs)

- Possible to have short brightening episode and repeat rarely → possible to be missed. → Background
- Asymmetric light curves, with a steep rise and a slow decline.
  - For some CVs, asymmetry is not seen due to gaps in light curve sampling or large photometric error bars
- Theoretical microlensing fit yields unphysical values (very large  $u_0$ , much brighter baseline fluxes than allowed by the reference images)
- 418 CVs in our sample from a visual inspection of light curves
  - Range from hours to months
  - None of CVs is left within  $0.3 < t_E < 2\text{days}$ .
  - No sample in same field found by other project (OGLE, MACHO-project).

# Background supernovae

- A kind sample of CVs (not repeat).
- Dominant background of survey toward the Large and Small Magellanic Clouds.
- Reject with means of asymmetric light curves same as CVs samples.
- The timescale is  $\sim 30$ days
  - Reject to require  $t_E < 2$ days (this target events).

# Binary microlensing

- Wide binary system : not background (clear separated)
- Close binary system and the mass of lens objects are far from the center mass → Two small caustics possible to be miss.
- Reject due to  $\chi^2$  value of fitting the data with close binary model.
  - For 9 events, Single lens model more favor than close binary model.
  - Only MOA-ip-5 cannot be rejected w/ this method (due to poor data point) → worse fit to binary than single. Unlikely to binary.

# Detection Efficiency

- Estimate efficiency w/ MC to compare Data/MC of  $t_E$  distribution.
- Artificial microlensing events were added at random positions in the observed images.
- The parameters of artificial events were uniformly generated at random in the following ranges:
  - $0 \leq u_0 \leq 1.5$ ,  $2453824 \leq t_0 \leq 2454420$  JD,  $0.1 \leq t_E \leq 250$  days,  $14.25 \leq I$  (source magnitude)  $\leq 21.15$  mag
  - The source magnitudes were weighted by the combined Luminosity function (LF) from MOA and the Hubble Space Telescope (HST).

# Detection Efficiency

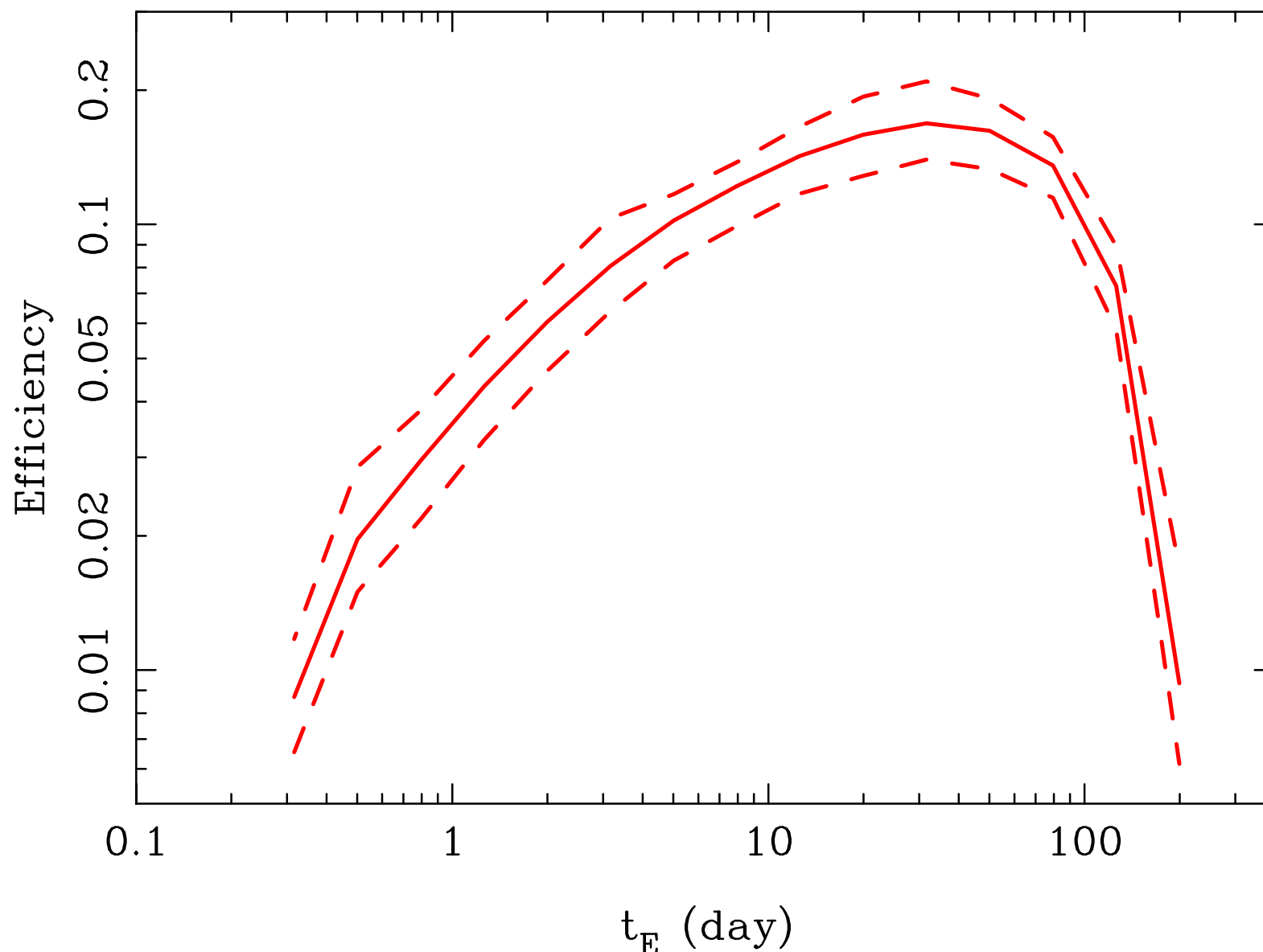
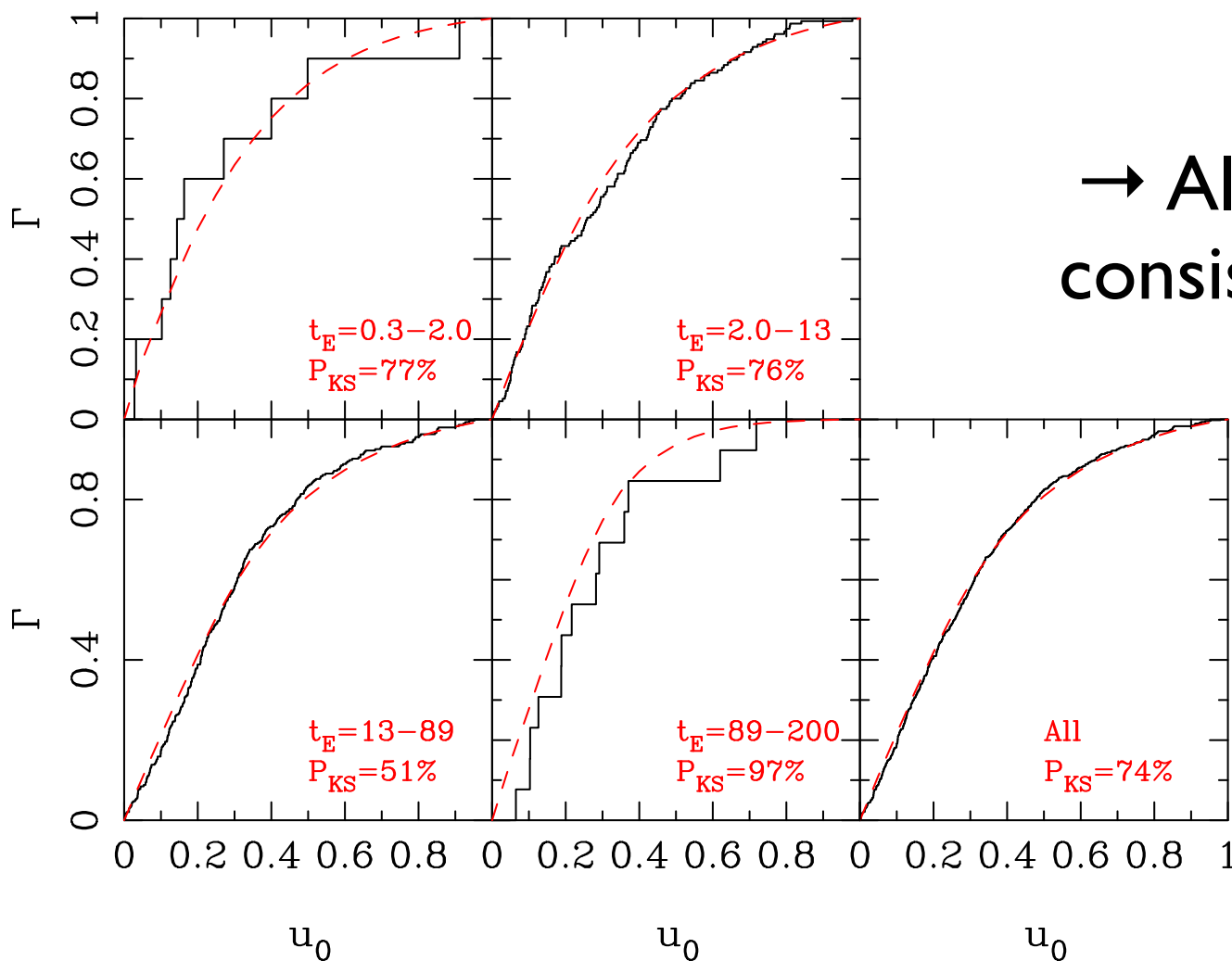


Figure S2.— The detection efficiencies of our experiment as a function of  $t_E$  for the source stars down to  $I = 20.0$  mag. Solid and dashed lines indicate the mean, minimum and maximum efficiencies of all fields.

# Systematic Bias

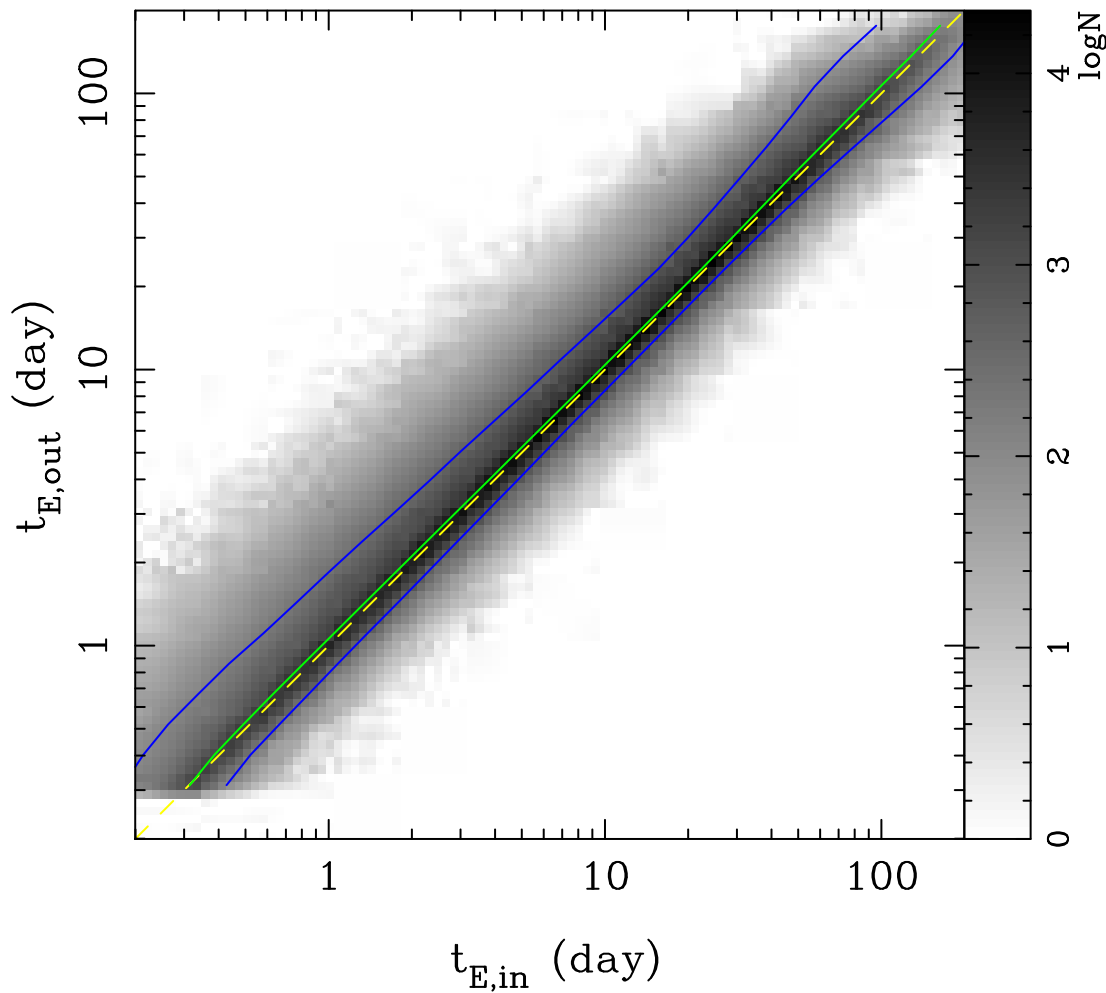
- Systematic bias for faint source or large photometric error.
- Check Data/MC of  $u_0$  consistency with Kolmogorov-Sirnov test.
- $u_0$  : purely geometric factor



→ All sub-sample  
consistent w/ MC.

# Systematic Bias

- Comparison b/w true  $t_E$  and reconstructed  $t_E$  w/ MC.
  - Small offset ( $t_{E,out} > t_{E,in}$ ), but not influent to this result.



# Likelihood analysis

- Constrain mass-function by likelihood  $L = \prod^{N_{\text{obs}}} \Phi(t_E, i) \times \varepsilon(t_E, i)$  to all (474) microlensing events.
  - $\Phi(t_E, i)$  :  $t_E$  distribution model (from MC for assumed stellar mass function w/ standard galactic mass density and velocity model)
  - Two mass functions : Power-law, log-normal
- $t_E < 2$  days, significant excess 10(data) / 1.5(power-law), 2.5(log-normal)  
→ 4e-6, 3e-4 (Poisson probabilities).
- **Add new planetary-mass  $\delta$  function model → Good fit**
  - $(M_{\text{pl}}/M_J, \Phi_{\text{pl}}) = (1.1^{+1.2}_{-0.6}, 0.49 \pm 0.13)$  of Power-law,  $(0.83^{+0.96}_{-0.51}, 0.46^{+0.17}_{-0.15})$  of log-normal → Planetary-mass  $\sim$  Jupiter-mass.
  - Imply  $1.9^{+1.3}_{-0.8}$  (power-low) and  $1.8^{+1.7}_{-0.8}$  (log-normal) times as many unbound or distant Jupiter-mass object as main-sequence stars

# Mass Function

#	Mass ( $M_{\odot}$ )	Function	parameter ( $M$ and $\sigma$ are in $M_{\odot}$ )	Fraction ( $N_*$ )
1	$40.0 \leq M$	Gaussian	Black hole ( $M_r = 5, \sigma_r = 1$ )	0.0031
	$8.00 \leq M \leq 40.0$	Gaussian	Neutron star ( $M_r = 1.35, \sigma_r = 0.04$ )	0.021
	$1.00 \leq M \leq 8.00$	Gaussian	White dwarf ( $M_r = 0.6, \sigma_r = 0.16$ )	0.18
	$0.70 \leq M \leq 1.00$	Power-law	$\alpha_1 = 2.0$	1.0
	$0.08 \leq M \leq 0.70$	Power-law	$\alpha_2 = 1.3$	
	$0.01 \leq M \leq 0.08$	Power-law*	$\alpha_3 = 0.48^{+0.29}_{-0.37}$ w/o PL	$0.73^{+0.22}_{-0.19}$
	$0.01 \leq M \leq 0.08$	Power-law**	$\alpha_3 = 0.50^{+0.36}_{-0.60}$ w/ PL	$0.74^{+0.30}_{-0.27}$
	$M = M_{PL}$	$\delta$ -function**	$M_{PL} = 1.1^{+1.2}_{-0.6} \times 10^{-3}, \Phi_{PL} = 0.49^{+0.13}_{-0.13}$	$1.9^{+1.3}_{-0.8}$
2	$40.0 \leq M$	Gaussian	Black hole ( $M_r = 5, \sigma_r = 1$ )	0.0031
	$8.00 \leq M \leq 40.0$	Gaussian	Neutron star ( $M_r = 1.35, \sigma_r = 0.04$ )	0.021
	$1.00 \leq M \leq 8.00$	Gaussian	White dwarf ( $M_r = 0.6, \sigma_r = 0.16$ )	0.18
	$0.08 \leq M \leq 1.00$	Log-normal*	$M_c = 0.12^{+0.03}_{-0.03}, \sigma_c = 0.76^{+0.27}_{-0.16}$	1.0
	$0.01 \leq M \leq 0.08$	Log-normal*	$M_c = 0.12^{+0.03}_{-0.03}, \sigma_c = 0.76^{+0.27}_{-0.16}$	$0.70^{+0.19}_{-0.30}$
	$0.00 \leq M \leq 0.01$	Log-normal*	$M_c = 0.12^{+0.03}_{-0.03}, \sigma_c = 0.76^{+0.27}_{-0.16}$	$0.17^{+0.24}_{-0.15}$
	$M = M_{PL}$	$\delta$ -function***	$M_{PL} = 0.83^{+0.96}_{-0.51} \times 10^{-3}, \Phi_{PL} = 0.46^{+0.17}_{-0.15}$	$1.8^{+1.7}_{-0.8}$

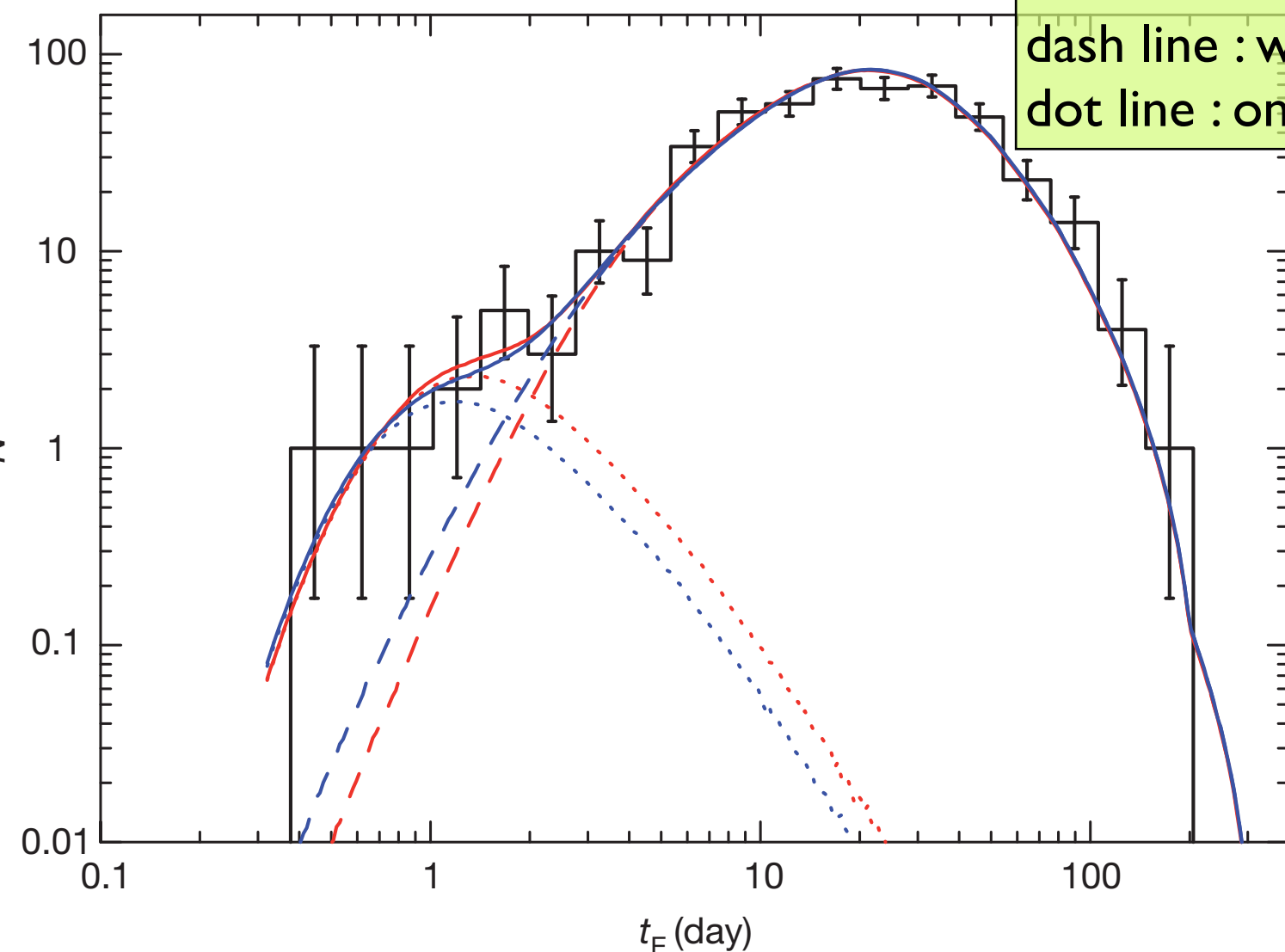
*Gaussian* :  $dN/dM = \exp[(M - M_r)^2 / 2\sigma_r^2]$

*Power law* :  $dN/d\log M = M^{1-\alpha}$       **Mc**: mean mass

*Log normal* :  $dN/d\log M = \exp[(\log M - \log M_c)^2 / 2\sigma_c^2]$

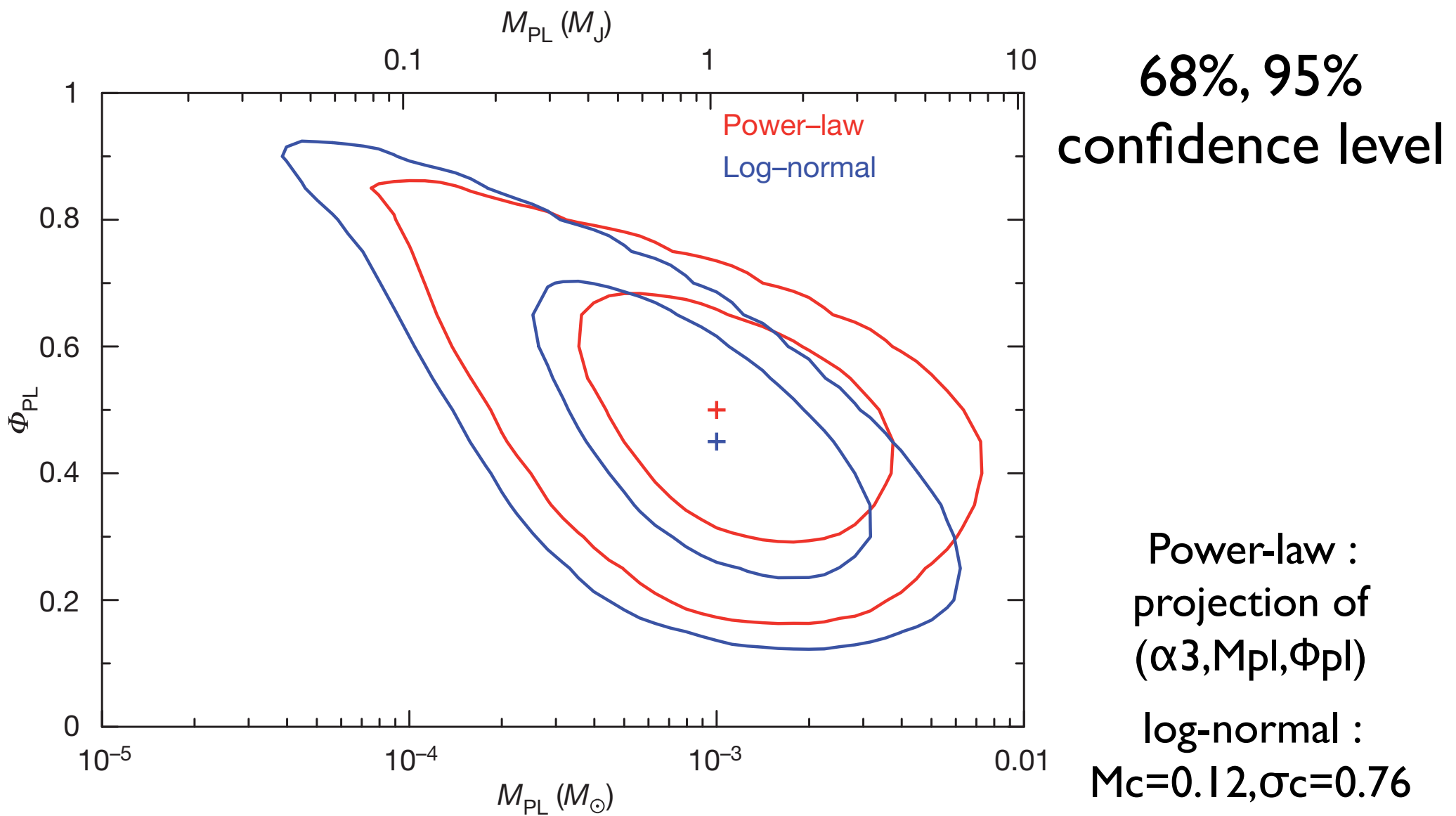
# Observed and theoretical $t_E$ distribution

With best-fit models



Black : 474 observed microlensing  
Red line : full power-law model  
Blue line : full log-normal model  
dash line : w/o  $\delta$ -function  
dot line : only  $\delta$ -function

# Likelihood contour for planetary- $\delta$ -mass function parameter



# Unbound/Distant

- Three set of planet and its host star events in this sample, which previously known (MOA, OGLE)
- Planets bound to host stars ( $\text{separation} < 10\text{-}20\text{AU}$ ) → Can detected as binary lens events.
  - Detect only single lens short events in this analysis.
- Fit to light curve of short events w/ binary light model to search the signature of host stars.
  - none of  $10 \text{ } t_E < 2\text{days}$  show any evidence.
- Estimate the upper limit of separation w/ Gemini Planet Imager data
  - # of Jupiter-mass object w/ semi-major axes of  $50\text{-}250 \text{ AU} < 30\%$  of all stars in Galactic Bulge.
  - 75% of observed “unbound/distant” planetary object (mass~1.8 Jupiter-mass) are not bound to any host stars.

# Conclusion

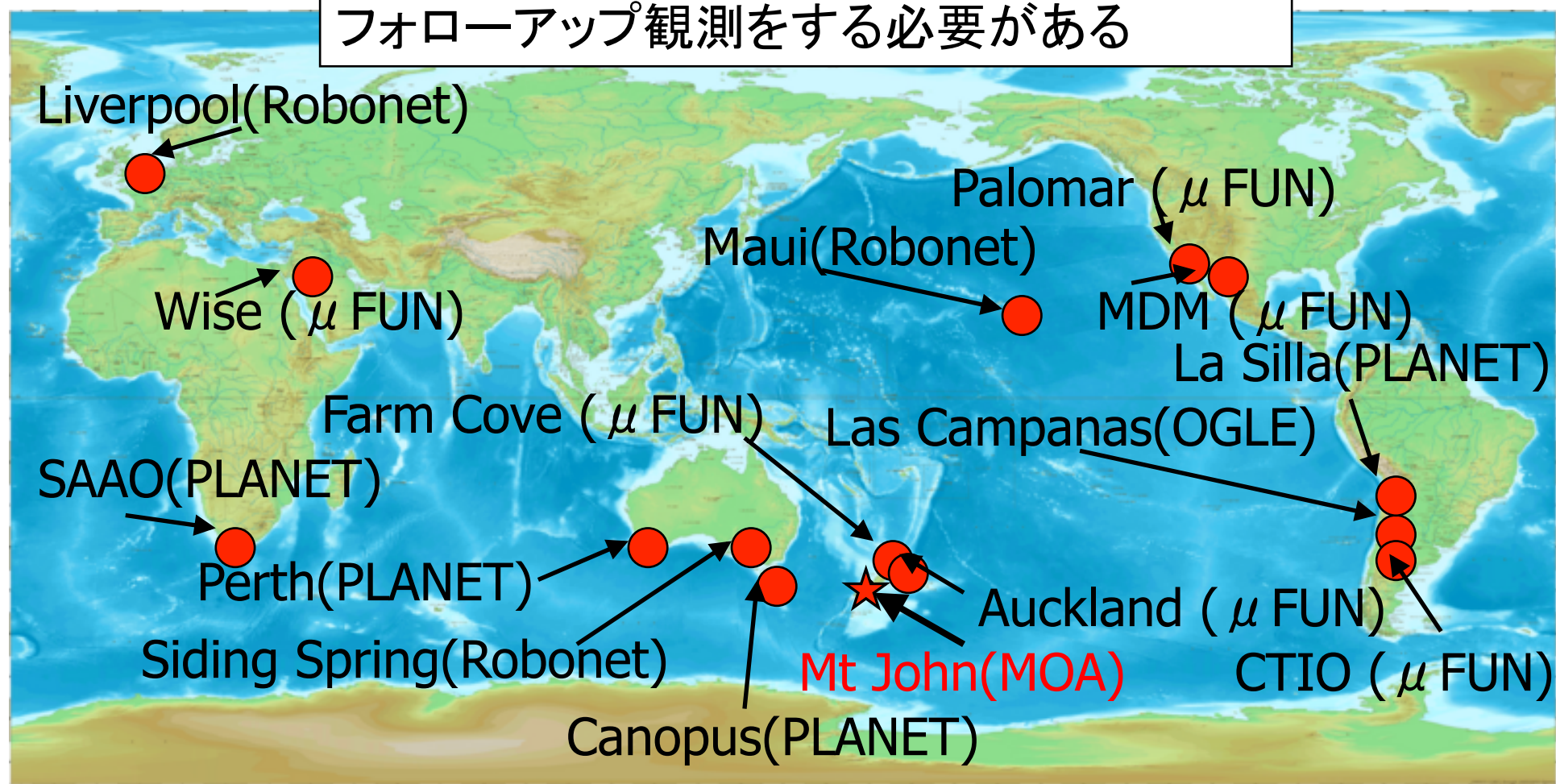
- Discovery almost twice unbound or distant Jupiter-mass object as many as main-sequence stars by gravitational microlensing.
- These objects are not bound to any host star.
- The observed planetary-mass population may have formed in protoplanetary disks at much smaller separations and been scattered into unbound or very distant orbits.

# Back up

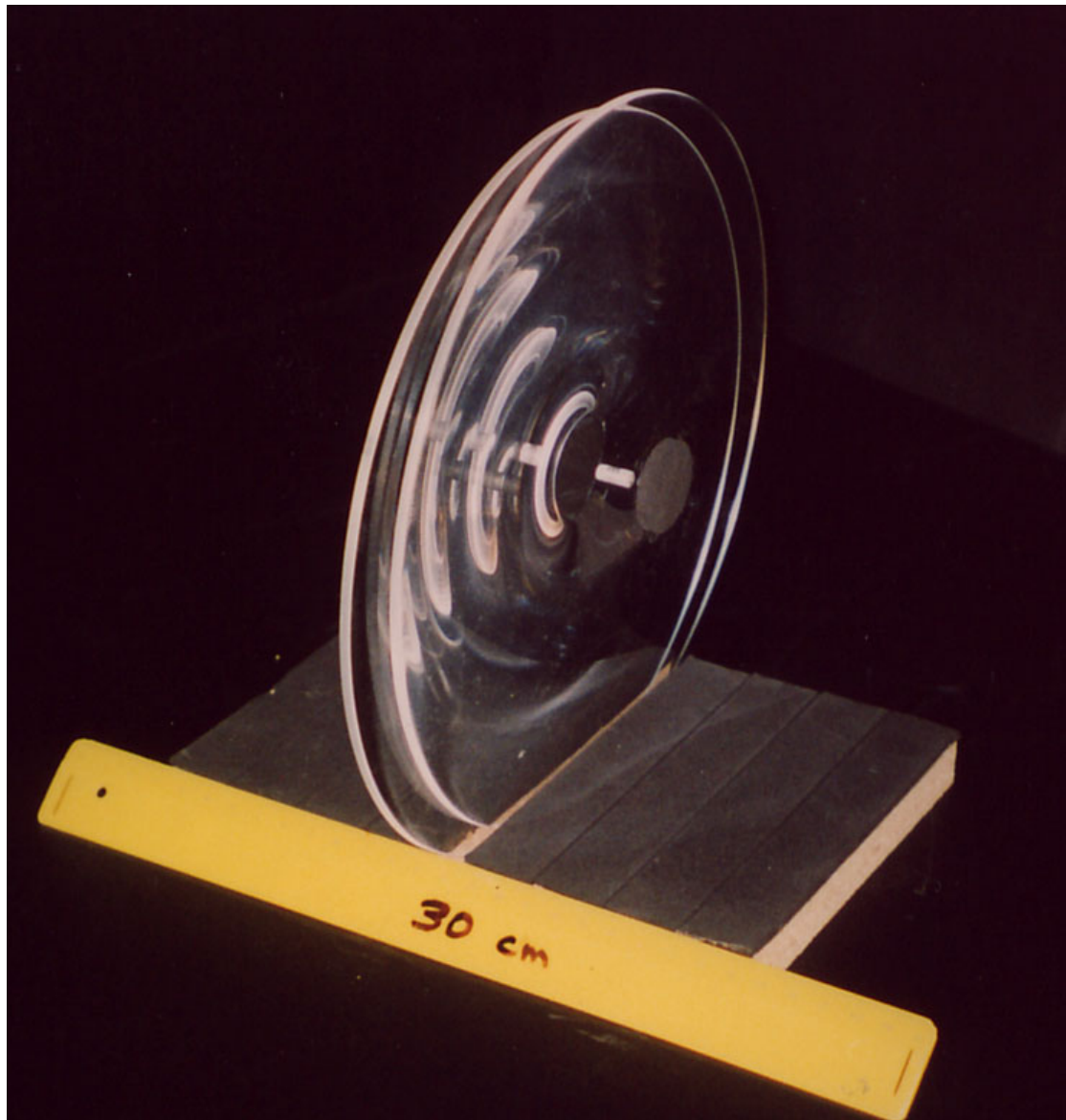
# マイクロレンズ観測ネットワーク

広視野望遠鏡 (MOA, OGLE) : サーベイとアラート  
小視野望遠鏡 (他グループ) : フォローアップ

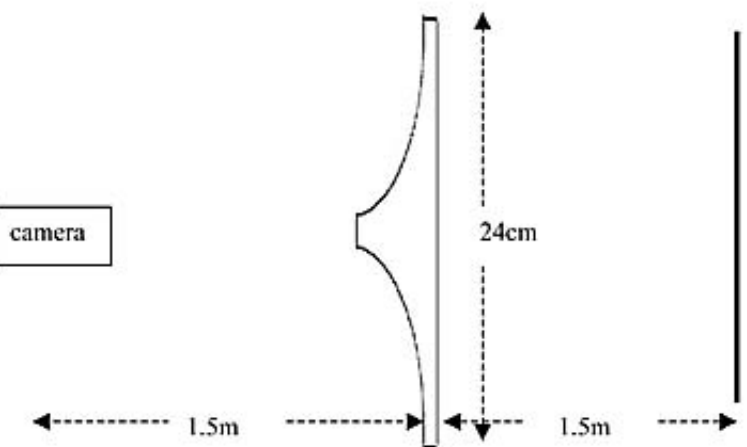
惑星イベントは短期間なのでリアルタイムで  
フォローアップ観測をする必要がある



# 重力レンズの実物



1. Microlensing demonstration



第2回『アインシュタインの物理』でリンクする研究・教育拠点研究会 (2009/10/23 大阪市立大学)

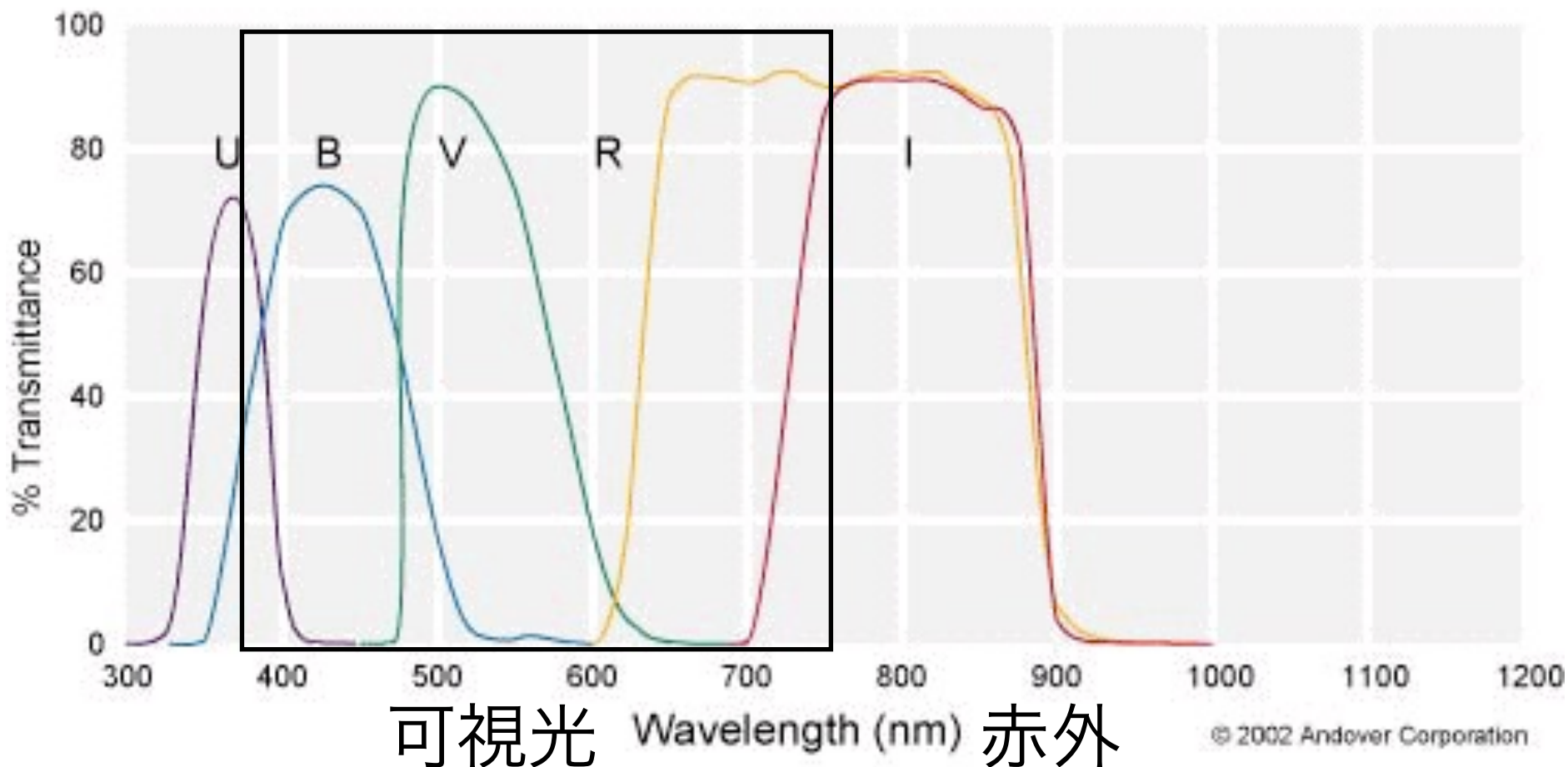
伊藤好孝「重力マイクロレンズ効果による暗天体」

# 重力マイクロレンズの増光マップ<sup>†</sup>



第2回『アインシュタインの物理』でリンクする研究・教育拠点研究会 (2009/10/23 大阪市立大学)

## Kron/Cousins UBVRI Filters

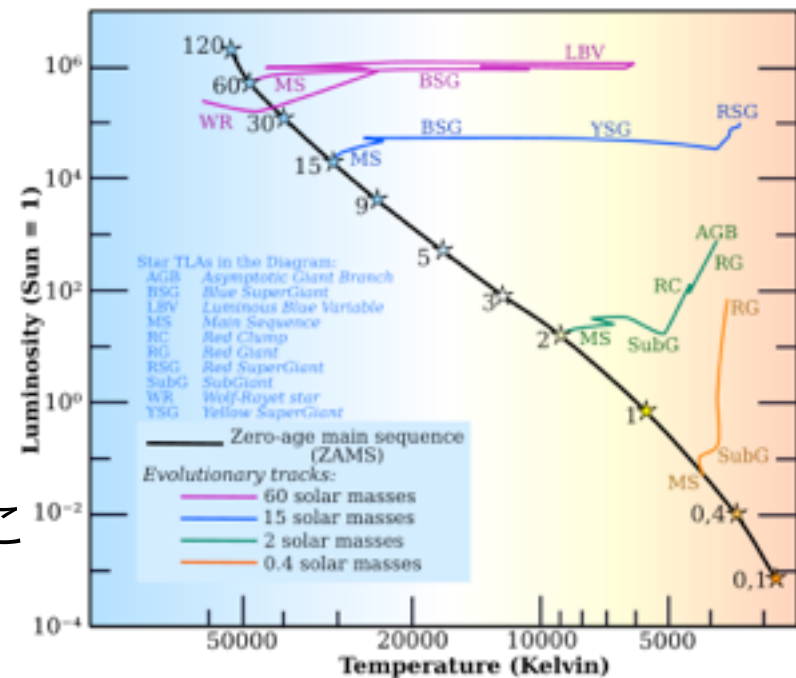


- U filter (P/N KRON-U-XX)
- B filter (P/N KRON-B-XX)
- V filter (P/N KRON-V-XX)
- R filter (P/N KRON-R-XX)
- I filter (P/N KRON-I-XX)

# Red clump

- レッドクランプ(Red clump)は、ヘルツシュフルング・ラッセル図で見られる特徴である。水平分岐の金属量が多い部分と考えられている。この領域の恒星はクランプ巨星と呼ばれることもあり、同じような表面温度の主系列星と比べて光度が大きい。ヘルツシュフルング・ラッセル図においては、主系列星の右上に位置する。主系列星が核の水素を燃やしているのに対して、恒星の進化におけるこの段階では、核のヘリウムを燃やしている。
- 理論上は、**レッドクランプの恒星の絶対光度は、恒星の組成や年齢とは関係なく、そのため銀河系内や隣の銀河との距離を測定するために都合の良い標準光源となっている。**

ヘルツシュフルング・ラッセル図



上図のRC=Red clump

# 補償光学 (adaptive optics)

- 大気のゆらぎをリアルタイムで補正する技術。
- 参照星と呼ばれる天体(観測天体、あるいはその近くの恒星)の波面を測定して、大気ゆらぎによって乱された波面を変形可能な鏡面によってリアルタイムに補正する技術。
- 一般的に、可視光波長で波面測定を行い、赤外波長で天体を観測する。
- 補正光学で補正された星像(PSF=Point Spread Function)は、中心部分(コア)、同心円状のリング(エアリーリング)、及びハローからなり、それらの割合は補正度合によって変わる。
- 望遠鏡の解像度の向上だけでなく、コアにエネルギーが集中することにより感度も向上する。惑星検出のためにハローを押える必要あり。

# Fast Moving objects

- PSF photometry at the fixed position where the variable object was first detected
- If an object moves a significant fraction of PSF, underestimate its brightness due to the off-center PSF.
  - the linear movement of such an object can produce a light curve which has some resemblance to a microlensing light curve
  - Such as an asteroid or Kuiper belt object, with a proper motion of  $\sim 1 \text{ arcsec h}^{-1}$ , can mimic a short timescale microlensing event
- Dust specs on the camera window can also produce similar light curves due to slight changes in the telescope pointing
- They generally give unphysical light curve parameters.
- Reject 3743 moving object in this data set due to poor microlensing fits or unphysical microlensing model parameters

# Microlensing by high velocity stars and Galactic halo stellar remnants

- Short timescale ( $t_E < 2\text{ days}$ ) events :
  - Small  $R_E$ , typical velocity
  - Typical  $R_E$ , high velocity
- $\langle t_E \rangle$  in galaxy bulge =  $\langle R_E \rangle / \langle v \rangle = \langle R_E \rangle / (\langle D \rangle \langle \mu \rangle) \sim 20\text{ days}$ 
  - $\mu > 10 \times \langle \mu \rangle \sim 60\text{ mas/yr} \Rightarrow t_E < 2\text{ days}$
- $6 \times 10^{-5}$  of stars in galaxy bulge with  $\mu \geq 60 \text{ mas/yr}$  (OGLE-II category)
  - Background rate < 0.01 (conservative)
- Stellar remnants (white dwarfs, neutron stars, black hole) sometime suggested as the microlensing events.
  - $\langle t_E \rangle > 20 \text{ days}, \langle v \rangle = 200\text{ km/s} \Rightarrow \text{Need } v \sim 2000\text{ km/s} > \text{Galactic escape velocity}$

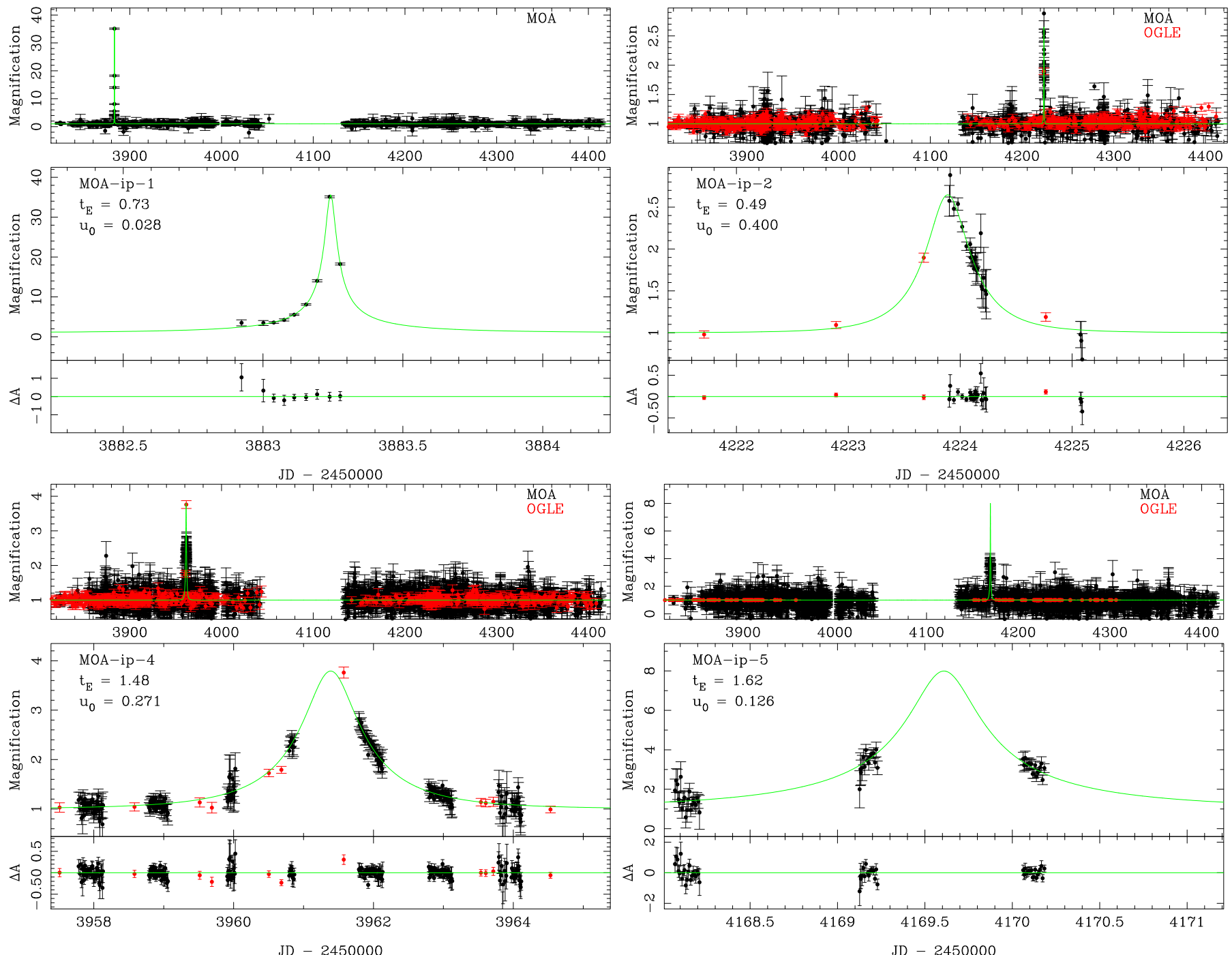
# Summary of observed events

**Table 1 | Microlensing parameters of short-timescale events**

ID	Field	Right ascension, $\alpha$ (2000)	Declination, $\delta$ (2000)	$N_{t_E}$	$t_0$ (JD')	$t_E$ (days)	$u_0$ ( $R_E$ )	$A_{\max}$	$I_s$ (mag)	$d_{\min}$ ( $R_{E^*}$ )
MOA-ip-1	gb1-4	17 h 46 min 24.506 s	-34° 30' 36.82''	9	3883.24171	0.73 ± 0.08	0.028 ± 0.003	35.6	19.7	7.0
MOA-ip-2	gb4-3	17 h 52 min 34.143 s	-30° 54' 14.25''	28	4223.88851	0.49 ± 0.10	0.400 ± 0.212	2.6	17.9	3.3
MOA-ip-3	gb5-7	17 h 54 min 58.325 s	-29° 38' 20.68''	170	4295.34720	1.88 ± 0.12	0.911 ± 0.096	1.4	17.2	3.6
MOA-ip-4	gb5-8	17 h 54 min 24.543 s	-29° 13' 29.39''	81	3961.38803	1.48 ± 0.12	0.271 ± 0.061	3.8	19.2	3.1
MOA-ip-5	gb9-2	17 h 57 min 17.008 s	-29° 02' 33.59''	69	4169.60907	1.62 ± 0.69	0.126 ± 0.159	8.0	19.2	2.4
MOA-ip-6	gb9-4	17 h 59 min 19.977 s	-29° 31' 24.70''	27	4189.49214	1.78 ± 0.24	0.499 ± 0.122	2.2	18.3	4.8
MOA-ip-7	gb9-5	17 h 57 min 36.678 s	-29° 59' 40.52''	51	4370.69496	1.82 ± 0.87	0.143 ± 0.125	7.0	19.4	5.2
MOA-ip-8	gb9-5	17 h 59 min 34.877 s	-30° 04' 24.04''	47	4013.14052	1.36 ± 0.15	0.103 ± 0.016	9.8	18.8	4.8
MOA-ip-9	gb10-5	17 h 57 min 52.952 s	-28° 16' 56.66''	16	3910.81772	0.96 ± 0.21	0.163 ± 0.058	6.2	19.5	3.4
MOA-ip-10	gb11-9	18 h 09 min 00.076 s	-32° 18' 39.91''	21	3932.99205	1.19 ± 0.04	0.032 ± 0.001	30.8	18.8	15.0

$N_{t_E}$  indicates the number of data points within  $t_0 \pm t_E$ , and  $t_0$ ,  $t_E$ ,  $A_{\max}$  and  $I_s$  indicate the time of peak magnification, the Einstein radius crossing time, the maximum magnification, and the source star magnitude of the best fit models of the MOA data, respectively.  $JD' = JD - 2,450,000$ .  $u_0$  and  $d_{\min}$  indicate the source-lens impact parameter and minimum host star separation in units of the Einstein radii of the planetary mass lens,  $R_E$ , and possible host star,  $R_{E^*}$ , respectively. The errors in  $t_E$  and  $u_0$  represent  $1\sigma$  limits,  $d_{\min}$  indicates  $2\sigma$  limits. MOA-ip-2, MOA-ip-3 and MOA-ip-10 were alerted as MOA-2007-BLG-144, MOA-2007-BLG-309 and MOA-2006-BLG-098 by the MOA real-time alert system (<http://www.massey.ac.nz/~iabond/moa>).

# Light curve of short microlensing events



# Light curve of short microlensing events

